Geophysical Research Letters

RESEARCH LETTER
10.1029/2022GL102392

Advances in Seasonal Predictions of Arctic Sea Ice With NOAA UFS

Jieshun Zhu[1], Wanqiu Wang[1], Yanyun Liu[1,2], Arun Kumar[1], and David DeWitt[1]

[1]Climate Prediction Center, NOAA/NWS/NCEP, College Park, MD, USA, [2]Earth Resources Technology Inc., Laurel, MD, USA

Key Points:

- This work is the first attempt with the Unified Forecast System (UFS) for seasonal predictions
- UFS presents better performance in seasonal prediction of Arctic sea ice than current operational systems at NOAA
- Better sea ice predictions with UFS are mainly related to its better representation of atmospheric states

Supporting Information:

Supporting Information may be found in the online version of this article.

Correspondence to:

J. Zhu,
jieshun.zhu@noaa.gov

Citation:

Zhu, J., Wang, W., Liu, Y., Kumar, A., & DeWitt, D. (2023). Advances in seasonal predictions of Arctic sea ice with NOAA UFS. *Geophysical Research Letters*, *50*, e2022GL102392. https://doi.org/10.1029/2022GL102392

Received 6 DEC 2022
Accepted 17 MAR 2023

© 2023. The Authors.
This is an open access article under the terms of the Creative Commons Attribution-NonCommercial-NoDerivs License, which permits use and distribution in any medium, provided the original work is properly cited, the use is non-commercial and no modifications or adaptations are made.

Abstract The Unified Forecast System (UFS) is the next generation modeling infrastructure under development for NOAA's operational numerical weather/climate predictions. This study is the first attempt with UFS for seasonal predictions application. In particular, 9-month hindcasts are performed starting from every month during 2007–2020. The UFS performance in predicting Arctic sea ice was compared to hindcasts by (a) the current operational Climate Forecast System version 2 (CFSv2) and (b) an experimental sea ice prediction system (CFSm5) at NOAA. Evaluations indicate that UFS demonstrates consistently improved skills than both CFSv2 and CFSm5 in seasonal sea ice predictions, together with more realistic climatological sea ice distributions. Diagnostics suggest that the better climatological sea ice distributions in UFS is related to its atmospheric states simulated with FV3, the atmospheric component of UFS, and reinforced by associated ocean circulations. In addition, applications of the multi-model ensemble strategy do not present skill improvements over the UFS forecasts alone.

Plain Language Summary Arctic sea-ice cover illustrates significant year-to-year fluctuations superimposed on the long-term decline trend. Seasonal forecasts of the ice interannual fluctuations could play an important role in providing planning information for shipping industries, improving management of ocean and coastal resources in the Arctic, and better serving Northern communities. In this study, we evaluated the capability of the Unified Forecast System (UFS) in predicting the Arctic sea ice coverage. The UFS is the next generation modeling infrastructure under development for NOAA's operational numerical weather/climate predictions, which has not been tried with seasonal predictions application before. Evaluations suggested that UFS demonstrates consistently improved skills in seasonal sea ice predictions than two systems currently in operations at NOAA, together with more realistic climatological sea ice distributions. Our further diagnostics suggest that the improvement is mainly related to the atmospheric states simulated with UFS, but is also reinforced by associated ocean circulations.

1. Introduction

The Unified Forecast System (UFS; https://ufscommunity.org) is a community-based, coupled, comprehensive earth modeling system under active developments in the US. It is designed to support the Weather Enterprise (https://www.weather.gov/about/weather-enterprise) and to be the modeling framework for NOAA's operational numerical weather/climate prediction applications, spanning local to global domains and predictive time scales from sub-hourly analyses to seasonal predictions. During its development, eight major UFS prototypes have been built and their performances were evaluated with reforecasts (https://registry.opendata.aws/noaa-ufs-s2s/). The prototypes differ in model resolutions/physics and initial conditions. The reforecasts are 35 days long and have been used for subseasonal predictability studies (e.g., Krishnamurthy et al., 2021). Yet few attempts have been made for seasonal predictions with UFS, which is an important aspect of NOAA's operational prediction practices.

A specific topic to be addressed in this study is seasonal predictions of Artic sea ice. The rapid loss of Arctic sea ice in recent decades, especially during the summer, has attracted growing interest in the predictability and prediction practices of sea ice on seasonal timescales. Accurate Arctic sea ice prediction is important for oil and shipping interests, wildlife protection, and ecosystems management. Predictability studies (e.g., Blanchard-Wrigglesworth et al., 2011; Day et al., 2014; Guemas et al., 2016) with a "perfect model" strategy suggested that the Arctic sea ice area (or extent) is potentially predictable about 1–2 years in advance and sea ice volume is about 3–4 years ahead. Assessments of actual sea ice predictions, on the other hand, show predictive skill out to only a few months

(e.g., Bushuk et al., 2017; Harnos et al., 2019; Wang et al., 2013). This gap has been attributed to errors in both model physics and initial conditions. As for the latter, for example, many efforts have been devoted to sea ice initializations (e.g., Blockley & Peterson, 2018; Collow et al., 2015, 2020; Zhang et al., 2022), and promising advances have been shown in sea ice predictions.

The NOAA/Climate Prediction Center (CPC) started issuing seasonal Arctic sea ice predictions in March 2015 for March to October starts each year, and extended to all months since November 2019. The latest CPC sea ice predictions are produced with a dynamical forecast system (CFSm5) modified from the operational Climate Forecast System version 2 (CFSv2) and a CPC Sea ice Initialization System (CSIS; Collow et al., 2020). Compared to the operational CFSv2, the modified system produces significant improvements for the ice melt season, but no improvements for the freeze-up season (Collow et al., 2020; Figure 2). In this study, we continue the effort toward better seasonal Arctic sea ice predictions by adopting the UFS. This will be the first attempt with the UFS for the practice of seasonal sea ice forecasts. Meanwhile, two model systems (i.e., UFS and a present prediction system CFSm5 at NOAA/CPC) with the same initialization strategy also provide an opportunity to explore the contribution of the model development to improved seasonal sea ice predictions.

This paper is organized as follows. The models, the experimental design and data sets are described in the next section. Section 3 presents our hindcasts and analyses. A summary and discussions are given in Section 4.

2. Models, Experiments and Data Sets

The coupled UFS model (https://ufscommunity.org) used in this study consists of the FV3 atmospheric component, the MOM6 oceanic component and the CICE6 sea ice component, and they are coupled through the Community Mediator for Earth Prediction Systems (CMEPS). The UFS version we use is Prototype 5. The FV3 resolution is C96 (~1°) horizontally with 64 vertical levels. The ocean and sea ice horizontal resolution is 0.25°. Relative to the default configuration of UFS, some cloud parameters adjustments in FV3 and the option of constant freezing temperature in CICE6 are adopted for a better Arctic sea ice representation (Y. Liu, Wang, et al., 2022).

The UFS hindcasts are initialized from 21st–25th of each month during 2007–2020 with one forecast run from each day, forming a five-member ensemble for each initial month, and cover 9 target months. In this paper, the first full month following initialization is referred as 0.5-month lead time, and so forth. For example, a February (March) prediction starting from 21st–25th January is defined as the prediction at the 0.5-month (1.5-month) lead. Their initial conditions are taken from the Climate Forecast System Reanalysis (CFSR; Saha et al., 2010) for the ocean, atmosphere and land, and from a MOM5-based CPC Sea Ice Initialization System (CSIS; Collow et al., 2020) for the sea ice. CSIS assimilates observational analyses of sea ice concentration (SIC; NASA Team SIC (Cavalieri et al., 1996)) and sea surface temperature (SST) (Reynolds et al., 2007) through a nudging method (Lindsay & Zhang, 2006).

The UFS performance in predicting Arctic sea ice at seasonal time scales is evaluated by comparing with hindcasts with CFSv2 (Saha et al., 2014; Wang et al., 2013) and CFSm5 (Collow et al., 2020) for which 10 and five ensemble members are respectively used in this study. CFSv2 is the present operational seasonal forecast system at NOAA, which was implemented in 2011. Its atmospheric component is the 2007 version of the NCEP operational GFS. It has a horizontal resolution at T126 with 64 vertical levels in a hybrid sigma-pressure coordinate, and its ocean component has a horizontal grid of 0.5×0.5 (with a meridional refinement near the equator) with 40 geopotential (z) levels. Its sea ice component is GFDL Sea Ice Simulator (SIS) model. In SIS, there are three layers including two equal layers of sea ice and one layer of snow; in each ice grid, there are five categories of possible sea ice thicknesses (0–0.1, 0.1–0.3, 0.3–0.7, 0.7–1.1, and greater than 1.1 m). It is initialized from the CFSR (Saha et al., 2010) for all model components. The CFSv2 hindcasts were performed every 5 days (Saha et al., 2014; Wang et al., 2013). In this study, 10 ensembles are constructed by using the 00z hindcasts with the first member taken as the first initial day around 11th of the first target month and subsequent members going backward every 5 days. The CFSm5 model is modified from CFSv2 with its oceanic component (MOM4) replaced with MOM5, and they have the same resolution for all components. Initial conditions and initialization dates for CFSm5 are the same as those for UFS. CFSm5 has been used to produce seasonal Arctic sea ice predictions routinely since May 2018 at the NOAA/CPC.

In this study, we will also assess the potential of the multi-model ensemble (MME) strategy for seasonal sea ice predictions, by combining (a) all three models (hereafter MME(all)), and (b) UFS and CFSm5 only (hereafter

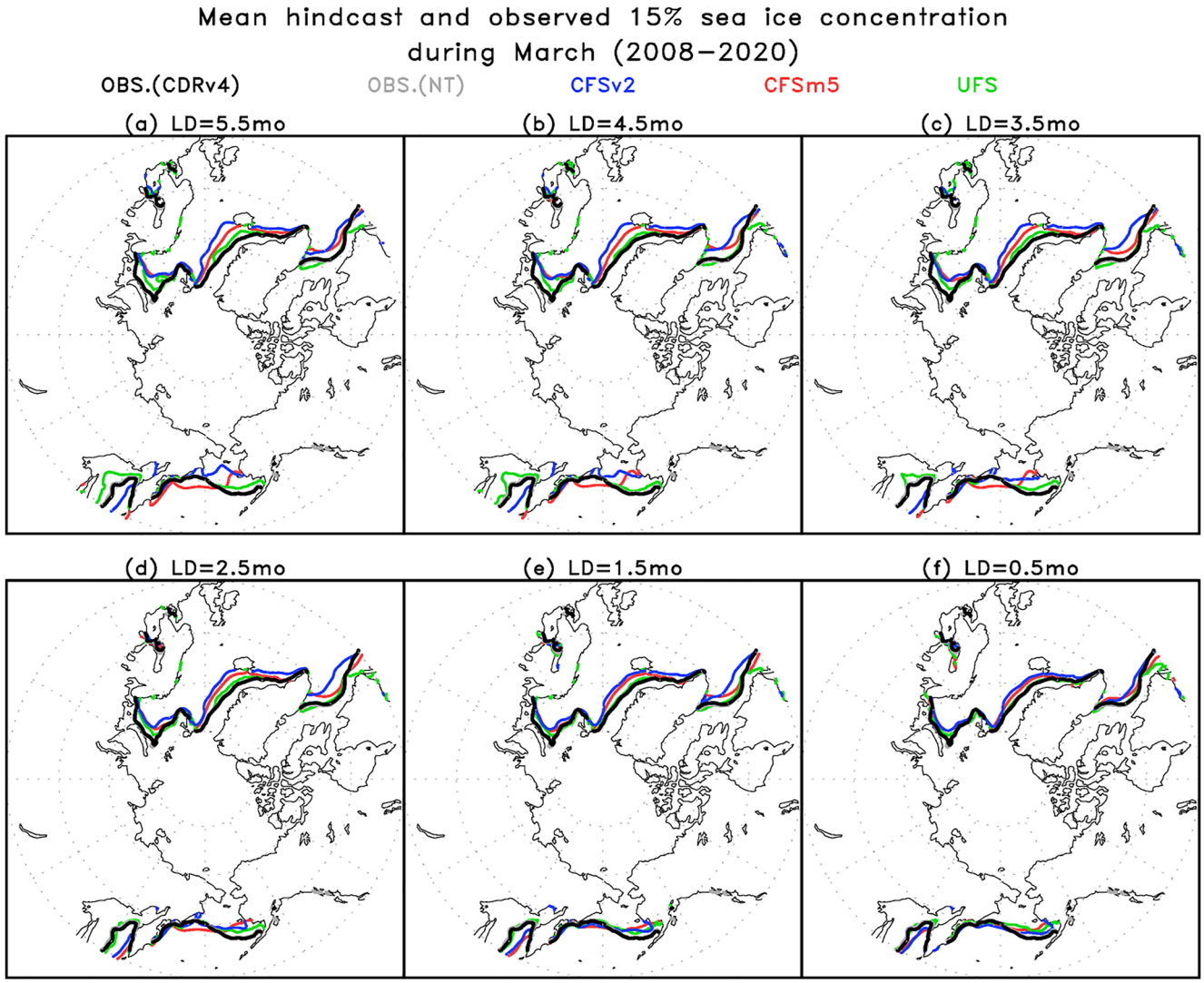

Figure 1. Climatology of 15% sea ice concentration during March in observations (black for CDRv4 and gray curves NASA Team), and hindcasts with Climate Forecast System version 2 (blue), CFSm5 (red), and Unified Forecast System (green). (a) For hindcasts starting from the prior September initial conditions during 2007–2020 (LD = 5.5 months), (b) for the prior October starts (LD = 4.5 months), (c) for the prior November starts (LD = 3.5 months), (d) for the prior December starts (LD = 2.5 months), (e) for the January starts (LD = 1.5 months), and (f) for the February starts (LD = 0.5 months).

MME(UFS + CFSm5)) in light of the obsolescence of CFSv2. The SIC from the NSIDC Climate Data Record version 4 (CDRv4; Meier et al., 2021) is used for verifications.

3. Results

We first examine the mean biases of sea ice coverage predicted with the three dynamical models. Figure 1 compares the mean 15% SIC contours (commonly used to define the sea ice coverage) during March at different lead times together with observational estimates with both CDRv4 and NASA Team analyses (which are almost identical). At the 0.5-month lead (predictions starting from February; Figure 1f), all contours overlap each other, indicative of small biases in all three models at the short lead. As the lead-time increases, the biases start to grow, especially for CFSv2 and CFSm5, and generally stabilize at the 3.5-month lead. On the Pacific side, excessive sea ice gradually builds up after the 0.5-month lead in the Sea of Okhotsk in both CFSv2 and CFSm5, and in the western Bering Sea in CFSm5. In the eastern Bering Sea, a too little sea ice coverage is shown in both CFSv2 and CFSm5, particularly in CFSv2 in which sea ice retreats almost to St. Lawrence Island south of the Bering Strait at the 5.5-month lead (the blue curve in Figure 1a). On the Atlantic side, both CFSv2 and CFSm5 produce too much

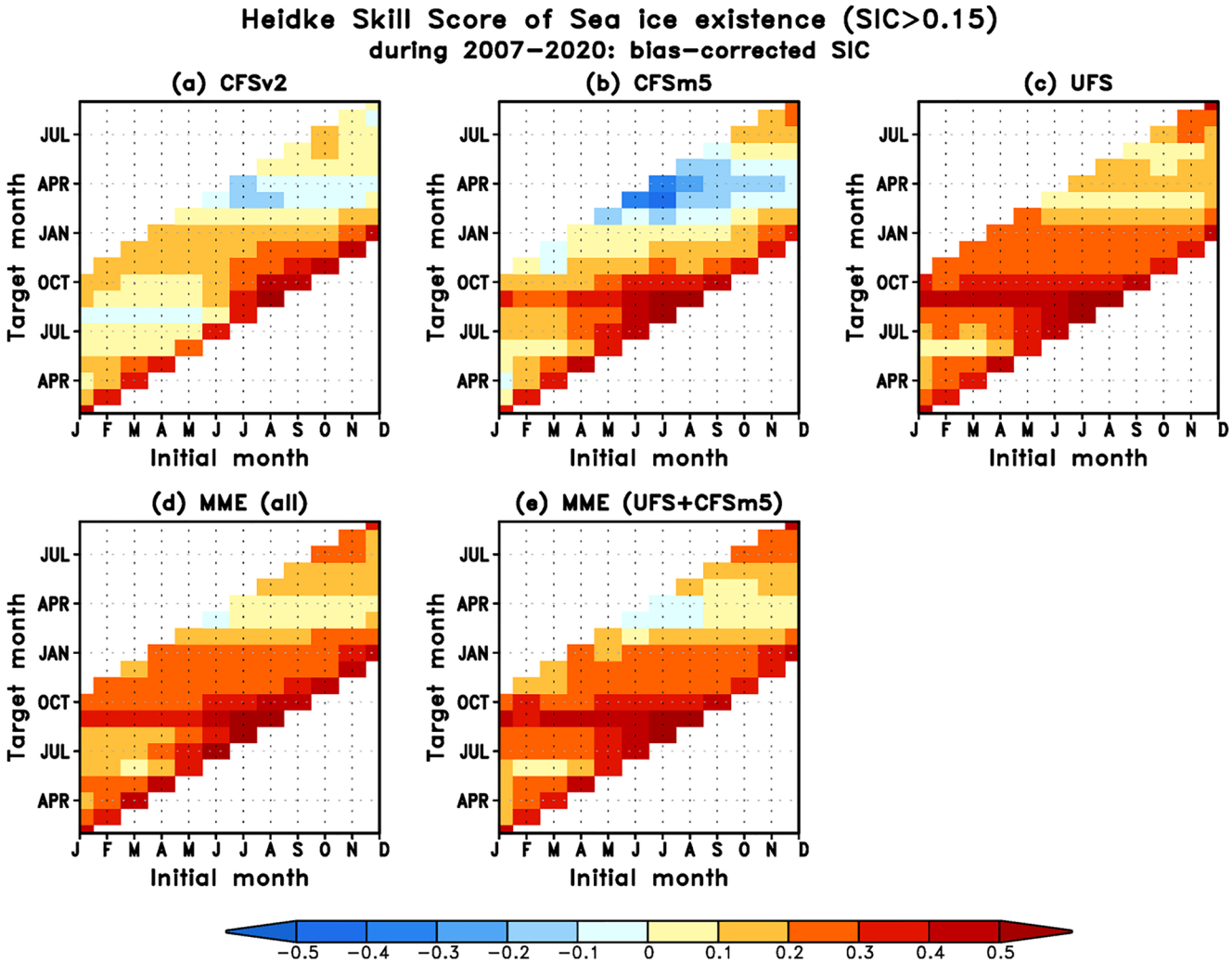

Figure 2. Heidke skill score of sea ice existence (SIC > 0.15) during 2007–2020 as a function of the initial month (*x*-axis; the month the forecast is started) and target month (*y*-axis; the forecast month) with (a) Climate Forecast System version 2, (b) CFSm5, (c) Unified Forecast System (UFS), (d) multi-model ensemble (MME) (all) and (e) MME (UFS + CFSm5).

sea ice coverage, and a larger bias is shown in CFSv2 again. In comparison, UFS produces a much more realistic sea ice coverage in the Arctic. Even at the 5.5-month lead (the green curve in Figure 1a), the sea ice edge of UFS follows the observed counterpart fairly well on both Pacific and Atlantic sides.

For summer (e.g., September in Figure S1 in Supporting Information S1), a too large sea ice coverage is present even at the 0.5-month lead in CFSv2 (blue curves in Figure S1f in Supporting Information S1), which was suggested to be related to biases in its sea ice initial conditions with CFSR (Collow et al., 2015, 2020). The bias grows further as forecast lead time increases, and the climatological sea ice distribution exaggeratedly extends to the Eurasian continent after the 1.5-month lead (blue curves in Figures S1a–S1e in Supporting Information S1). For CFSm5 and UFS, the forecasted edges of sea ice overlap each other at 0.5- and 1.5-month leads, suggesting a dominant impact of initial conditions on sea ice forecasts at the short leads during summer as they are initialized from the same CSIS system. As lead time increases, the sea ice coverage starts diverging between CFSm5 and UFS with too much (little) sea ice coverage in CFSm5 (UFS), but their biases seem comparable in magnitude between CFSm5 and UFS and are clearly smaller than those in CFSv2 (Figures S1a–S1d in Supporting Information S1).

Next, seasonal forecast skills of Arctic sea ice are evaluated with a Heidke-type skill score (HSS). The HSS metric is calculated based on the forecast of existence or non-existence of sea ice. Sea ice is considered to exist

in forecasts or observations if the SIC is greater than 15%. The HSS is calculated for each forecast month, and is defined as

$$\mathrm{HSS} = \frac{AC - AC_e}{AT - AC_e},$$

where AC is the total area of correct forecast, AC_e is total area of expected correct forecasts based on observed climatological states defined during 1991–2020, and AT is the total area of all grid boxes being considered (poleward of 55.25°N with land grid boxes excluded). A positive (negative) HSS value indicate a better skill of the model forecast than the forecast based on observed climatology.

Figure 2 compares HSS metrics in all three model hindcasts and two MMEs for different target and initial seasons, averaged over 2007–2020. Overall, in all models the forecast skills of Arctic sea ice are dependent more on the forecast target month than the initial month, and lowest skill tends to occur during late winter and spring. For CFSv2, however, essentially no skill is shown for the summer period with the HSS values near zero from June to September in the forecast initialized from January to May. The problem has been attributed to the CFSv2 initialization with unrealistic CFSR SIT, and can be significantly alleviated with better initial SIT conditions (Collow et al., 2015, 2020). Compared to CFSv2, CFSm5 presents significant improvements in predicting sea ice melt in the Arctic (Collow et al., 2020), in which HSS reaches 0.4 when predicting sea ice minimum in September. On the other hand, it is noted that both CFSv2 and CFSm5 have difficulties in predicting sea ice coverage during late winter and spring in which their HSS values are mostly negative. Compared to CFSv2 and CFSm5 (Figures 2a and 2b), UFS (Figure 2c) presents a substantial skill increase for all target seasons. In particular, HSS in UFS is above 0.4 in predicting sea ice minimum in September, slightly better than CFSm5 and significantly better than CFSv2. The skill improvement with UFS is even more evident for the freeze-up season during which HSS is uniformly above zero (0.1–0.2).

The potential of the MME strategy in seasonal sea ice predictions is further assessed by combining the model hindcasts. It is noted that the skill of UFS forecasts does not improve from the inclusion of CFSm5 and/or CFSv2 (Figure 2c vs. Figures 2d and 2e) forecasts. As a matter of fact, its skill during winter degrades for the MME with a reduction in the HSS from 0.1 to 0.2 to around 0. This conclusion is different from prior MME practices (e.g., Dirkson et al., 2019; Harnos et al., 2019) which demonstrated a beneficial effect of MME on seasonal sea ice predictions. Our calculations seem to suggest that the MME strategy might not help improve sea ice forecasts if skills of component forecasts diverge greatly.

The above contrast in skill in predicting the sea ice melt can be better seen for specific events. Figure S2 in Supporting Information S1, as an example, demonstrates SIC anomalies during July 2019 in both the CDRv4 observational estimate and hindcasts starting from May 2019. Overall, both UFS (Figure S2d in Supporting Information S1) and CFSm5 (Figure S2c in Supporting Information S1) captured the pattern of observed anomalies (Figure S2a in Supporting Information S1) very well, such as the positive anomalies in Chukchi Sea and Beaufort Sea and the negative anomalies along the southern edge of the Arctic in the Atlantic side. The positive anomalies in Baffin Bay and Davis Strait and around Prince Charles Island are also well captured by UFS and CFSm5. The prediction performance is not further improved with the MME strategy no matter whether CFSv2 is included or not (Figures S2e and S2f in Supporting Information S1). In contrast, CFSv2 failed to capture the observational pattern, and instead predicted positive SIC anomalies all along the edge of the Artic (Figure S2b in Supporting Information S1).

In the above skill assessments (e.g., Figure 2), the model SICs have been bias-corrected by removing lead time-dependent climatologies. In light of the reduction of mean biases of sea ice in the UFS (Figure 1), it will be interesting to know if the prior practice of bias corrections is still necessary for seasonal sea ice predictions. Figure 3 is the same as Figure 2 but based on SICs predicted by models without bias corrections. It is noted that the skill superiority of UFS becomes even more evident: it is not only significantly better than CFSv2 and CFSm5, but also superior to two MMEs (particularly for the freeze-up season). However, skills for all predictions are lower than that with bias corrections (Figure 2). Even in UFS which has the highest prediction skill, the HSS values are mostly negative except for September sea ice minimum at all lead times or for a few other target months at 0.5-month lead. The low prediction skill based on raw forecast data suggests that bias corrections are still critical in seasonal sea ice predictions in spite of great advances in representing sea ice with the contemporary model systems.

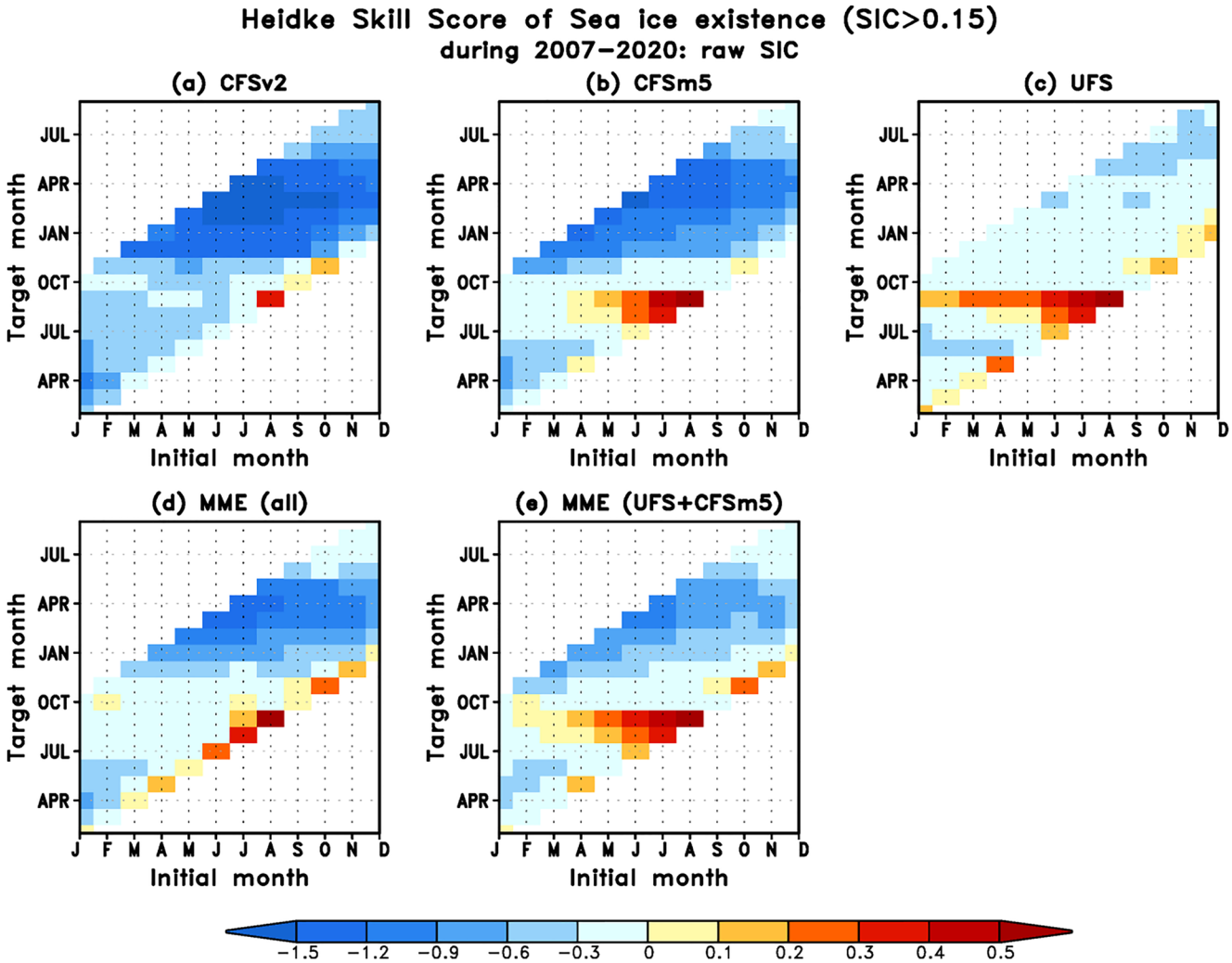

Figure 3. As in Figure 2, but based on sea ice concentrations directly predicted by models (with no bias corrections applied). Note that the displaying scales for negative Heidke-type skill scores are tripled relative to those in Figure 2.

The importance of bias corrections in seasonal sea ice predictions also implies that the better prediction skill with UFS might result from its better representation of climatological sea ice distributions. Therefore, to understand why UFS has a better sea ice prediction skill, we next explore which processes contributed to its better climatological sea ice distribution. Since the CFSm5 and UFS hindcasts are initialized in a same way for all model components, a comparison between them allows us to focus on the effect of model system, and is more straightforward than comparisons against the CFSv2 hindcasts which will be complicated by additional influence from initialization differences. Specifically, we will compare CFSm5 and UFS forecasts starting from November and May, in which forecasts at the 3.5-month lead correspond to March and September, respectively. As discussed above about Figure 1 and Figure S1 in Supporting Information S1, the sea ice coverage biases in both CFSm5 and UFS reach a saturation at the 3.5-month lead for both March and September.

We first look at the build-up of sea ice coverage difference during March. Figure 4a–4c show the differences in predicted atmospheric 10-m winds and the surface net downward heat flux, and oceanic surface currents between CFSm5 and UFS during the season prior to March, that is, December to February (DJF). (We focus on differences between CFSm5 and UFS outputs rather than comparisons with observation-based estimates, because our objective is to illustrate differences between these two systems and observational uncertainties also tend to be relatively large in the Arctic.) For the surface net heat fluxes (Figure 4b), over the central Arctic, the lower boundary (i.e., sea ice) in CFSm5 releases more heat fluxes into the atmosphere than in UFS. Over the ice-edge regions where the existence of sea ice is more sensitive to external forcing, the lower boundary in CFSm5 releases more heat

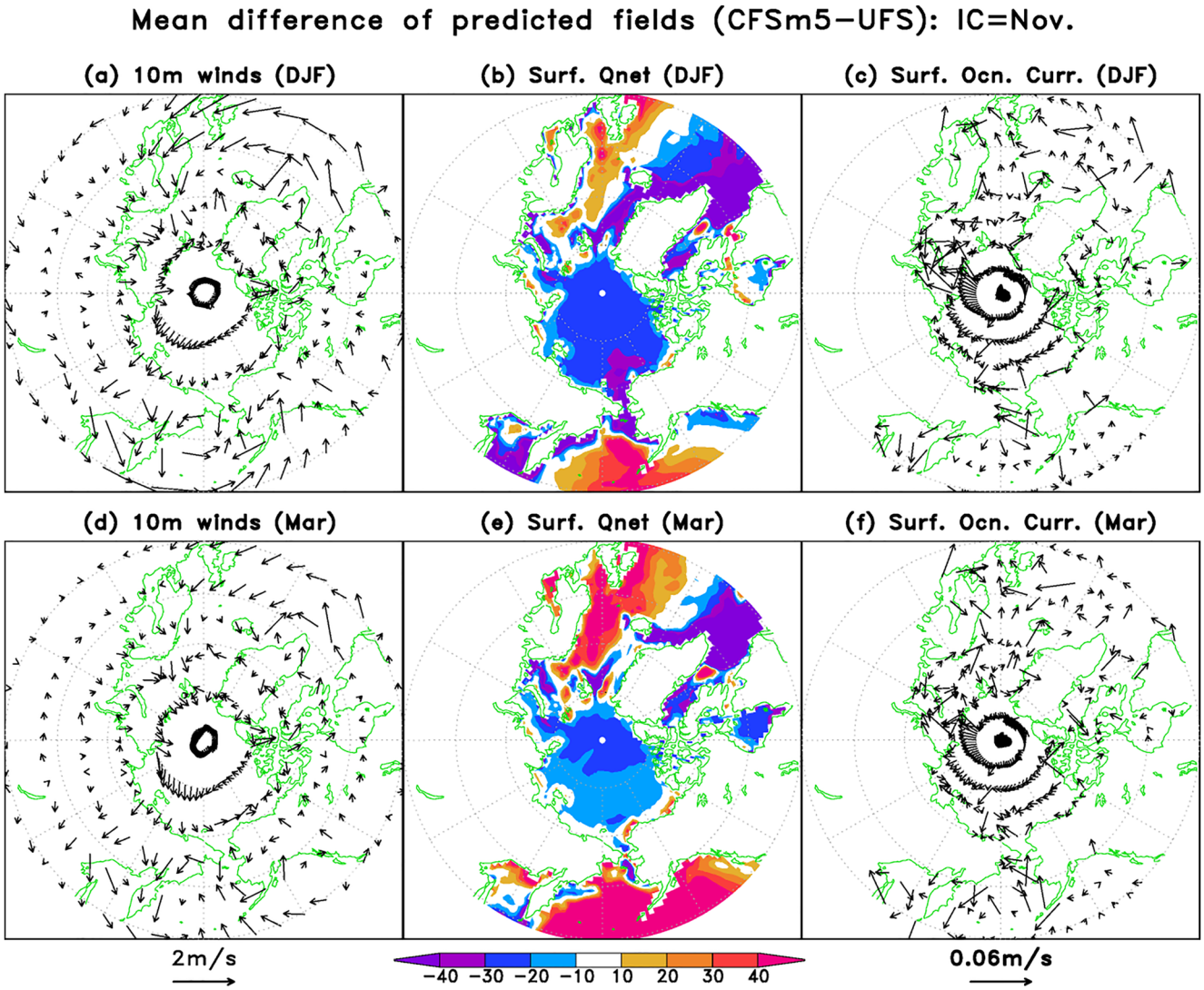

Figure 4. Mean difference of predicted fields between CFSm5 and Unified Forecast System (UFS) starting from November initial conditions during (a–c) DJF and (d–f) March. (a, d) For 10-m winds (m/s), (b, e) for net heat fluxes (W/m^2) at surface, and (c, f) for surface ocean currents (m/s). The difference shown is calculated as CFSm5 minus UFS.

fluxes than in UFS over the Sea of Okhotsk, the far western Bering Sea, Baffin Bay and east of Greenland, but less heat fluxes in the eastern Bering Sea. The heat flux distributions are consistent with the distributions of differences in sea ice coverage between CFSm5 and UFS (e.g., Figure 1), suggesting that the thermodynamic forcing is contributing to the gradual build-up of larger sea ice coverage biases in CFSm5.

Meanwhile, dynamic processes appear to have contributions as well. For instance, around the Bering Sea, the low-level atmosphere (Figure 4a) features a cyclonic structure difference between CFSm5 and UFS, with southerly (northerly) wind difference in the eastern Bering Sea (in the western Bering Sea and the Sea of Okhotsk). The wind structure differences favor a northward retreat (a southward expansion) of sea ice coverage in CFSm5 in the eastern Bering Sea (in the western Bering Sea and the Sea of Okhotsk). Furthermore, in response to the wind difference, oceanic surface circulation difference between CFSm5 and UFS builds up as well in this region (Figure 4c), and the current difference seems to play a similar role as surface winds, reinforcing the sea ice coverage difference between CFSm5 and UFS (red and green curves in Figure 1). Contributions from similar dynamic processes can also be seen in some regions on the Atlantic side, for example, east of Greenland.

When reaching March (Figure 4d–4f), the overall atmospheric and oceanic structures are similar to those during DJF, and thereby continue to sustain the sea ice coverage difference between CFSm5 and UFS afterward

(Figure 1). One minor difference between March and DJF (Figure 4d–4f vs. Figure 4a–4c) is that heat flux difference becomes less consistent with sea ice coverage differences during March, suggesting that dynamic processes might start to play a larger role in sustaining the sea ice coverage difference.

During September when CFSm5 has a larger sea ice coverage than UFS (Figure S1 in Supporting Information S1), the physics behind these differences seem simpler than during March. Figure S3 in Supporting Information S1 compares atmospheric and oceanic states between CFSm5 and UFS forecasts starting from May. It is seen that, around the ice edge in the Arctic, the lower boundary (ocean/ice) in CFSm5 releases more heat fluxes into the atmosphere than in UFS during both June–August (JJA) and September (Figures S3b and S3e in Supporting Information S1), but differences in surface winds (Figures S3a and S3d in Supporting Information S1) or currents (Figures S3c and S3f in Supporting Information S1) are small. It suggests that the sea ice coverage difference between CFSm5 and UFS is mainly caused and sustained by thermodynamic processes during September.

Overall, the above analyses suggest that a better climatological sea ice distribution in UFS is mainly related to its atmospheric states simulated with its atmospheric component—FV3, through both thermodynamic and dynamical processes. For the winter season, the atmospheric effect is also reinforced by associated ocean circulations, which, however, are at least partially driven by the overlying winds.

4. Conclusion and Discussions

This study represents a first attempt with the UFS for seasonal prediction application. In particular, we performed a set of 9-month seasonal hindcasts initialized from every month during 2007–2020. Arctic sea ice is a specific focus in this paper, and its seasonal prediction skill with the UFS was compared to those made by the current NOAA operational system CFSv2 and an experimental system CFSm5. Comparisons indicate that the UFS demonstrates a clear improvement in the climatological sea ice distribution in the Arctic and a significantly better capability in predicting Artic sea ice existence at the seasonal timescale. During the freeze-up season, for instance, while the prediction skill with both CFSv2 and CFSm5 is substantially worse than a prediction based on climatological sea ice information, the merit of UFS is evident with its HSS reaching 0.1–0.2.

Further, the MME strategy and bias corrections are evaluated for seasonal sea ice predictions. It is found that the skill of UFS forecasts cannot be further improved by combining predictive information from CFSm5 and/or CFSv2 with UFS. Bias corrections, however, are found to be critical for predictions of Arctic sea ice at the seasonal timescale, although contemporary models like the UFS have presented significant improvements in sea ice simulations.

The conclusion regarding bias corrections also indicates a critical role of climatological sea ice distributions in seasonal sea ice predictions. Therefore, we further explored the physics contributing to climatological sea ice distributions, by leveraging the existing hindcasts with UFS and CFSm5, which were initialized in a same way for all their model components. It was found that a better climatological sea ice distribution in UFS is mainly related to its atmospheric states simulated with its atmospheric component—FV3, in which both thermodynamic and dynamical processes play an important role. This finding is consistent with some recent studies which suggested that the observed Arctic sea ice variability is primarily driven by atmospheric processes (e.g., Z. Liu, Risi, et al., 2022). On the other hand, for the winter season, the atmospheric effect can also be reinforced by associated ocean circulations, which, however, are at least partially driven by the overlying winds. We expect that additional experiments in future studies will help further clarify the impacts of errors in the atmospheric models, for example, forcing the ocean and sea ice components of UFS and CFSm5 with observed surface fields and model produced surface fields from UFS and CFSm5 hindcasts.

Data Availability Statement

Data used in this study are all public resources. In particular, NSIDC CDRv4 sea ice concentrations are available through Meier et al. (2021). SST data is available through Reynolds et al. (2007). CFSR data is available through Saha et al. (2010) (https://www.avl.class.noaa.gov/saa/products/search?sub_id=0&datatype_family=CFS-R&-submit.x=21&submit.y=9). Sea ice concentrations from our hindcasts are available through https://www.cpc.ncep.noaa.gov/products/people/jszhu/data4paper/GRL23seaice.tar.gz.

Acknowledgments
The authors thank Dr. Hui Wang, Dr. Thomas Collow, and anonymous reviewers for their insightful comments. This work is supported by the NWS Office of Science and Technology Integration (OSTI) program. We thank the EMC Dynamics and Coupled Modeling Group for their help with the configuration of the UFS. Forecast runs were carried out on the NOAA's R&D HPC System GAEA. The scientific results and conclusions, as well as any view or opinions expressed herein, are those of the author(s) and do not necessarily reflect the views of NWS, NOAA, or the Department of Commerce.

References

Blanchard-Wrigglesworth, E., Armour, K. C., Bitz, C. M., & DeWeaver, E. (2011). Persistence and inherent predictability of Arctic sea ice in a GCM ensemble and observations. *Journal of Climate*, *24*(1), 231–250. https://doi.org/10.1175/2010JCLI3775.1

Blockley, E. W., & Peterson, K. A. (2018). Improving Met Office seasonal predictions of Arctic sea ice using assimilation of CryoSat-2 thickness. *The Cryosphere*, *12*(11), 3419–3438. https://doi.org/10.5194/tc-12-3419-2018

Bushuk, M., Msadek, R., Winton, M., Vecchi, G., Gudgel, R., Rosati, A., & Yang, X. (2017). Skillful regional prediction of Arctic sea ice on seasonal timescales. *Geophysical Research Letters*, *44*(10), 4953–4964. https://doi.org/10.1002/2017gl073155

Cavalieri, D. J., Parkinson, C. L., Gloersen, P., & Zwally, H. (1996). *Sea ice concentrations from Nimbus-7 SMMR and DMSP SSM/I-SSMIS passive microwave data*. National Snow and Ice Data Center.

Collow, T. W., Liu, Y., Wang, W., & Kumar, A. (2020). Overview of the CPC Sea Ice initialization system (CSIS) and its use in experimental sea ice forecasting at the NOAA climate prediction center. In *Extended summary, climate prediction S&T digest, 44th NOAA climate diagnostics and prediction workshop, Durham, NC, 22–24 October 2019, DOC/NOAA* (pp. 85–88). https://doi.org/10.25923/t4qa-ae63

Collow, T. W., Wang, W., Kumar, A., & Zhang, J. (2015). Improving Arctic sea ice prediction using PIOMAS initial sea ice thickness in a coupled ocean-atmosphere model. *Monthly Weather Review*, *143*(11), 4618–4630. https://doi.org/10.1175/MWR-D-15-0097.1

Day, J. J., Tietsche, S., & Hawkins, E. (2014). Pan-Arctic and regional sea ice predictability: Initialization month dependence. *Journal of Climate*, *27*(12), 4371–4390. https://doi.org/10.1175/JCLI-D-13-00614.1

Dirkson, A., Denis, B., & Merryfield, W. (2019). A multimodel approach for improving seasonal probabilistic forecasts of regional Arctic sea ice. *Geophysical Research Letters*, *46*(19), 10844–10853. https://doi.org/10.1029/2019gl083831

Guemas, V., Blanchard-Wrigglesworth, E., Chevallier, M., Day, J. J., Deque, M., Doblas-Reyes, F. J., et al. (2016). A review on Arctic sea ice predictability and prediction on seasonal-to-decadal timescales. *Quarterly Journal of the Royal Meteorological Society*, *142*(695), 546–561. https://doi.org/10.1002/qj.2401

Harnos, K., L'Heureux, M., Ding, Q., & Zhang, Q. (2019). Skill of seasonal Arctic sea ice extent predictions using the North American Multi-model Ensemble. *Journal of Climate*, *32*(2), 623–638. https://doi.org/10.1175/jcli-d-17-0766.1

Krishnamurthy, V., Meixner, J., Stefanova, L., Wang, J., Worthen, D., Moorthi, S., et al. (2021). Sources of subseasonal predictability over CONUS during boreal summer. *Journal of Climate*, *34*(9), 3273–3294. https://doi.org/10.1175/JCLI-D-20-0586.1

Lindsay, R. W., & Zhang, J. (2006). Assimilation of ice concentration in an ice-ocean model. *Journal of Atmospheric and Oceanic Technology*, *23*(5), 742–749. https://doi.org/10.1175/jtech1871.1

Liu, Y., Wang, W., Yang, W., Zhu, J., Kumar, A., & DeWitt, D. (2022). Evaluation of subseasonal Arctic sea ice hindcasts in an NCEP's UFS-based system. In *Extended summary, climate prediction S&T digest, 46th NOAA climate diagnostics and prediction workshop, virtual online, DOC/NOAA* (pp. 32–35). https://doi.org/10.25923/rj6c-rk11

Liu, Z., Risi, C., Codron, F., Jian, Z., Wei, Z., He, X., et al. (2022). Atmospheric forcing dominates winter Barents-Kara sea ice variability on interannual to decadal time scales. *Proceedings of the National Academy of Sciences of the United States of America*, *119*(36), e2120770119. https://doi.org/10.1073/pnas.2120770119

Meier, W. N., Fetterer, F., Windnagel, A. K., & Stewart, J. S. (2021). *NOAA/NSIDC climate data record of passive microwave sea ice concentration, version 4*. NSIDC: National Snow and Ice Data Center. https://doi.org/10.7265/efmz-2t65

Reynolds, R. W., Smith, T. M., Liu, C., Chelton, D. B., Casey, K. S., & Schlax, M. G. (2007). Daily high-resolution blended analyses for sea surface temperature. *Journal of Climate*, *20*(22), 5473–5496. https://doi.org/10.1175/2007jcli1824.1

Saha, S., Moorthi, S., Pan, H. L., Wu, X., Wang, J., Nadiga, S., et al. (2010). The NCEP climate forecast system reanalysis. *Bulletin of the American Meteorological Society*, *91*(8), 1015–1057. https://doi.org/10.1175/2010BAMS3001.1

Saha, S., Moorthi, S., Wu, X., Wang, J., Nadiga, S., Tripp, P., et al. (2014). The NCEP climate forecast system version 2. *Journal of Climate*, *27*(6), 2185–2208. https://doi.org/10.1175/JCLI-D-12-00823.1

Wang, W., Chen, M., & Kumar, A. (2013). Seasonal prediction of arctic sea ice external from a coupled dynamical forecast system. *Monthly Weather Review*, *141*(4), 1375–1394. https://doi.org/10.1175/MWR-D-12-00057.1

Zhang, Y.-F., Bushuk, M., Winton, M., Hurlin, B., Delworth, T., Harrison, M., et al. (2022). Subseasonal-to-seasonal sea ice forecast skill improvement from sea ice concentration assimilation. *Journal of Climate*, *35*(13), 4233–4252. https://doi.org/10.1175/jcli-d-21-0548.1